

## SEARCH FOR DIFFUSE COSMIC GAMMA RAYS ABOVE 200 TeV

J. MATTHEWS, D. CIAMPA, K. D. GREEN, J. KOŁODZIEJCZAK, D. NITZ, D. SINCLAIR,  
 G. THORNTON,<sup>1</sup> AND J. C. VAN DER VELDE

Department of Physics, Randall Laboratory, University of Michigan, Ann Arbor, MI 48109

AND

G. L. CASSIDAY, R. COOPER, S. C. CORBATO, B. R. DAWSON,<sup>1</sup> J. W. ELBERT, B. E. FICK, D. B. KIEDA, S. KO,  
 D. F. LIEBING,<sup>2</sup> E. C. LOH, M. H. SALAMON, J. D. SMITH, P. SOKOLSKY, S. B. THOMAS, AND B. WHEELER

Department of Physics, University of Utah, Salt Lake City, UT 84112

Received 1990 July 16; accepted 1990 December 28

### ABSTRACT

We have searched for  $\gamma$ -rays in the cosmic radiation above 200 TeV using a two-level array of scintillators. Surface counters measure the size and direction of extensive air showers while counters buried 3 m below the ground are used to measure their muon content in detail. We find no evidence for an excess number of muon-poor showers and conclude that  $\gamma$ -rays comprise less than 0.4% of all cosmic rays above 200 TeV and less than 0.05% above 1000 TeV (90% CL). The muon content of showers from the direction of the Galactic disk is the same as that of showers from other regions of the sky. The ratio of the flux of Galactic  $\gamma$ -rays to that of cosmic rays is less than  $8.0 \times 10^{-5}$  (90% CL). This limit, based on muon measurements, represents a significant improvement over previous experiments and approaches predicted levels for diffuse  $\gamma$ -rays from the Galactic plane.

*Subject headings:* cosmic rays: general — gamma rays: general

### 1. INTRODUCTION

The origin of ultra high energy (UHE,  $> 10^{14}$  eV) cosmic rays is a long-standing problem. Neutral particles such as  $\gamma$ -rays should provide tracers of cosmic rays since their trajectories are undeflected by interstellar magnetic fields. For example, if UHE protons are accelerated in the vicinity of neutron star binary systems and interact with accreting or enshrouding material, then UHE  $\gamma$ -rays are likely to result. Regardless of whether such compact sources of UHE  $\gamma$ -rays exist, the interaction of the highest energy cosmic rays with the cosmic background radiation or with interstellar gas would generate diffuse fluxes of  $\gamma$ -rays.

Two distinct kinds of diffuse  $\gamma$ -ray fluxes can occur and are characterized by their arrival directions. Depending upon the production mechanism, one type of diffuse flux will appear isotropic while the other will be concentrated along the Galactic disk.

If UHE cosmic rays are of extragalactic origin an isotropic flux of  $\gamma$ -rays will result from the interaction of cosmic-ray protons above  $10^{19}$  eV with the cosmic background radiation (CBR) through interactions such as

$$p\gamma^* \rightarrow pe^+e^-, \quad p\gamma^* \rightarrow p\pi^0, \quad \pi^0 \rightarrow \gamma\gamma,$$

where  $\gamma^*$  represent CBR photons. The secondary  $e^+$ ,  $e^-$  and  $\gamma$ -rays encounter other CBR photons over intergalactic distances and subsequently cascade. An enhanced flux of  $\gamma$ -rays piles up near  $10^{14}$  eV where the cascades terminate near the threshold for  $\gamma\gamma^* \rightarrow e^+e^-$  (Berezinsky & Kudryavtsev, 1988, 1990; Halzen et al. 1990; Yoshida & Teshima 1990).

A flux of  $\gamma$ -rays from the direction of the Galactic disk

should arise from interactions of primary cosmic rays on gas and dust. The intensity of these  $\gamma$ -rays relative to the cosmic-ray flux is expected to diminish above  $10^{15}$  eV (Berezinsky & Kudryavtsev 1988, 1990). The distribution of  $\gamma$ -rays should reflect the distribution of interstellar material. In the 30 MeV to 5 GeV regime, photons produced in this manner have been observed by *COS B* and *SAS 2* satellites and have been used to map the density of Galactic hydrogen (Hartman et al. 1979; Mayer-Hasselwander et al. 1982).

In a review of older data, Clay, Protheroe, & Gerhardy (1984) found no evidence for UHE  $\gamma$ -rays from the Galactic plane and placed an upper limit on the ratio of the flux of  $\gamma$ -rays to that of ordinary hadronic cosmic rays of  $I_\gamma/I_{CR} < 1.5\%$ . More recent work by the BASJE Collaboration at Mount Chacaltaya reports (Suga et al. 1988) similar limits above 180 TeV and, in older data, the possibility of a few  $\gamma$ -events above 100 TeV at a level of  $I_\gamma/I_{CR} \approx 6 \times 10^{-4}$ . A positive signal of the same strength has also been reported by the Tien-Shan group based on eight events from directions away from the Galactic plane (Nikolskii, Stamenov, & Ushev 1987). At lower energies (1 TeV), the Whipple Observatory group (Reynolds et al. 1990) reports no Galactic  $\gamma$ -rays at the 1% level.

We have searched for diffuse  $\gamma$ -ray emission using the muon content of extensive air showers to distinguish  $\gamma$ -ray-induced events. Measurement of muons in extensive air showers sensitively discriminate  $\gamma$ -rays from the ordinary cosmic-ray background since muons are copiously produced in hadronic air showers but are relatively rare in showers initiated by  $\gamma$ -rays. The validity of this approach is based on the assumption that UHE  $\gamma$ -rays have interaction properties which can be extrapolated from lower energies.

Following the work of Samorski & Stamm (1983), there have been some hints that muon production in  $\gamma$ -showers is somehow enhanced (for a review, see Protheroe 1987). This has become one of the outstanding questions of cosmic-ray and

<sup>1</sup> Department of Physics, University of Adelaide, Adelaide, South Australia 5001, Australia.

<sup>2</sup> WSRL, Defence Science and Technology Organization, Salisbury, South Australia, Australia.

particle physics. Most theoretical attempts to significantly increase the number of muons in  $\gamma$ -ray air showers have failed. The experimental evidence remains inconclusive. The conventional picture of  $\gamma$ -ray interactions is therefore the best framework in which to attempt to observe UHE  $\gamma$ -rays. Observation of diffuse fluxes of  $\gamma$ -rays by means of muon discrimination would confirm the standard model of muon photoproduction and provide a valuable "test beam" with which to calibrate the muon content of  $\gamma$ -showers.

## 2. EVENT SELECTION AND DETERMINATION OF SHOWER SIZE AND DIRECTION

The Utah-Michigan array is located at Dugway, Utah, at the site of the Fly's Eye installation ( $40^\circ\text{N}$ ,  $113^\circ\text{W}$ , atmospheric depth  $870 \text{ g cm}^{-2}$ ). This experiment is the first stage of the Utah-Michigan-Chicago (UMC) experiment and operated from late 1987 until 1990 February 20. As shown in Figure 1, there are 33 counter stations on the surface distributed within a circle of 100 m radius and 512 counters arranged in eight patches buried 3 m below the surface. The counters on the surface measure the size and direction of each shower while the buried counters sample the muons. A surface station has an area of  $1.5 \text{ m}^2$  and consists of four slabs of scintillator each viewed by two photomultiplier tubes (PMTs). A patch of buried counters contains 64 sheets of scintillator each  $2.5 \text{ m}^2$  in area, 0.64 cm thick, and viewed by a single 5" PMT at its center. Measurements taken with overlapping scintillators showed that the buried counters detected muons with an efficiency of 93% (Sinclair 1989).

The experiment operated with from four to eight patches of muon counters in 1988. Eight muon patches (512 counters) were operational in 1989 and 1990, having a total area of buried counters of  $1280 \text{ m}^2$ . This is the largest muon detector ever employed in an air shower array.

An event is recorded when at least seven surface stations and

15 or more surface counters report hits within  $2 \mu\text{s}$ . The buried array does not participate in the event trigger so there is no bias with regard to the muon content of recorded showers.

For each surface station we record which counters were hit, the time of the first hit, and the total energy deposition in the four counters in that station. These data are used to calculate the direction and total charged particle size  $N$  at the ground for each shower. The method proceeds in five steps:

1. An approximate direction is found by fitting the arrival times to a plane-front.
2. The position of the shower's core is estimated by calculating a weighted average of the pulse heights from each station.
3. The shower size  $N$  and a better measurement of the core coordinates are found by a least-squares fit of the particle densities to the following lateral distribution function:

$$\rho(x) = Nkx^{-0.7}(1+x)^{-3.2}, \quad (1)$$

where  $\rho(x)$  is the measured density of particles at position  $x = r/r_1$ ,  $r$  is the distance from the core,  $r_1 = 80 \text{ m}$ , and  $k$  is the normalization constant such that

$$\int_0^\infty \rho 2\pi r dr = N.$$

This is equivalent to the Nishimura-Kamata-Greisen lateral distribution function (Greisen 1960) of fixed shower age  $s = 1.3$ .

4. An improved direction is found by a least-squares fit of arrival times to a conical shower front whose apex is at the core.

5. Finally, an improved value for the shower's size is found by adjusting the parameter  $N$  and using a maximum likelihood method to compare the measured particle densities to equation (1).

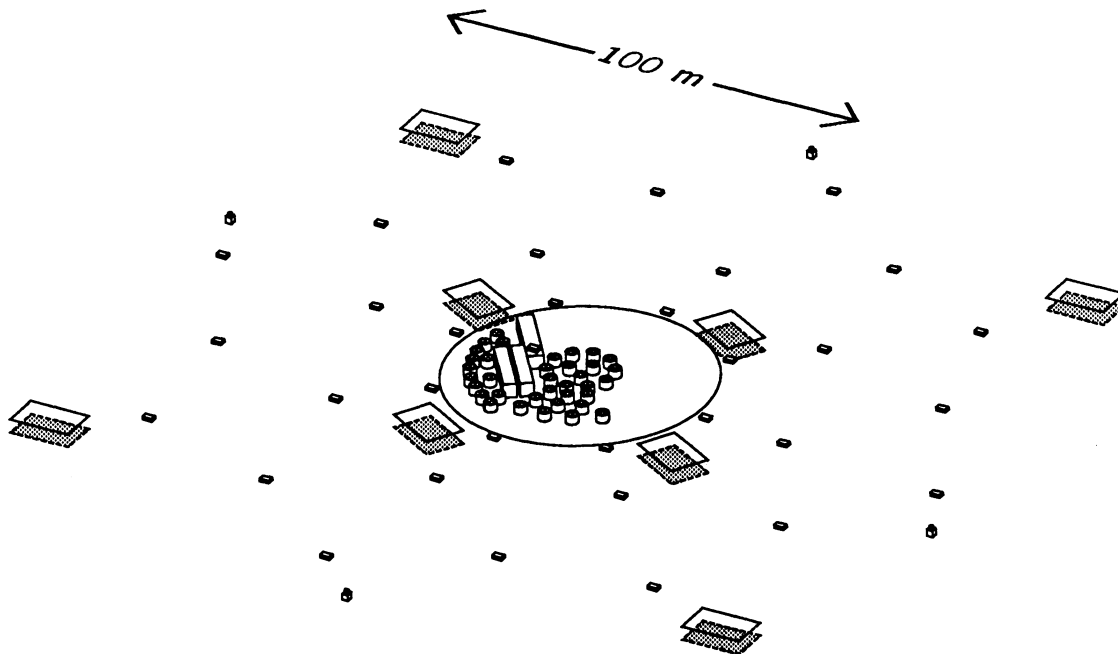


FIG. 1.—Elevated view of the Utah-Michigan array. The shaded rectangles indicate eight 64 counter muon patches. The smaller rectangles show positions of the 33 unit surface array. The Fly's Eye II installation and electronics trailers are shown at the center.

The accuracy of the fitted direction is estimated by three independent methods: simulations, comparison to data obtained by a tracking air-Cerenkov telescope operated in coincidence with the array, and from the data itself by dividing the array into two parts and fitting each half separately. For showers with  $N > 3 \times 10^4$  whose cores are within 100 m of the center of the array,  $\delta\theta = 3^\circ$  where  $\delta\theta$  would contain 72% of the events from a point source. Systematic pointing error is less than  $0.3^\circ$ .

The onset of the trigger causes some loss of showers with  $N < 5 \times 10^4$ . Saturation of the surface stations cause an underestimation of the number of particles in showers with  $N > 10^6$ . In what follows, the data are restricted to showers whose sizes lie in the range  $3 \times 10^4 < N < 10^6$ , cores within 100 m of the center of the array, and directions within  $40^\circ$  of the zenith. We retain  $1.9 \times 10^7$  events by these criteria.

The minimum energy of showers above a minimum size is not sharply defined. The relationship between mean size and primary energy varies with zenith angle, and there are fluctuations in size at a particular energy. We define the threshold energy  $E_\gamma$  as the energy at which our acceptance of  $\gamma$ -showers reaches 25% of its maximum value for showers with declinations  $30^\circ < \delta < 50^\circ$ . For example, we estimate, based on simulations, that we would retain 25% of  $\gamma$ -showers of energy  $E_\gamma = 200$  TeV when the requirement  $N > 3 \times 10^4$  is imposed. For an incoming flux  $\phi_\gamma(>E_\gamma) \propto E_\gamma^{-1.0}$  this energy is very nearly the median energy of the retained set (Ciampa et al. 1990). The energy distribution of accepted showers is nearly unchanged for assumed spectral indices from 1.0 to 1.7 (the spectral index of cosmic-ray protons). If the size cut is increased to  $N > 3 \times 10^5$ , the corresponding energy threshold increases to 1000 TeV.

We note that, at our altitude, vertical protons, and  $\gamma$ -rays of the same energy will produce air showers of very nearly the same size at the ground. Consequently, the energy distribution of accepted proton-showers will be similar to that of  $\gamma$ -showers as described above.

### 3. MUON CONTENT OF AIR SHOWERS

The muons associated with each shower are sampled by the buried counters. We record the arrival time for each of the buried counters that has been hit by one or more particles ("hits") but not the number of particles hitting an individual counter. The time window for accepting pulses from the muon counters is  $\pm 55$  ns for the inner four patches of counters and  $\pm 100$  ns for the outer four, relative to the arrival times of the shower front at each of the patches as computed from surface array data.

The buried counters which have not been hit ("misses") also provide information about the muon content of the shower. The total muon size  $N_\mu$  is found by a maximum likelihood fit which compares the hits and misses to a standard lateral distribution function (Greisen 1960):

$$\rho_\mu(x) = N_\mu k_\mu x^{-0.75}(1+x)^{-2.5}, \quad (2)$$

where  $k_\mu$  is the normalization constant for the muons,  $x = r/r_0$ ,  $r$  is the distance from the core, and  $r_0 = 300$  m. We use the core position and shower direction determined by the surface array data.

We assume that showers of all sizes and slant angles can be fitted to a single lateral distribution function by adjusting only the size parameter  $N_\mu$ . We use the data to test this assumption. In Figure 2 we compare the lateral distributions of hits in the

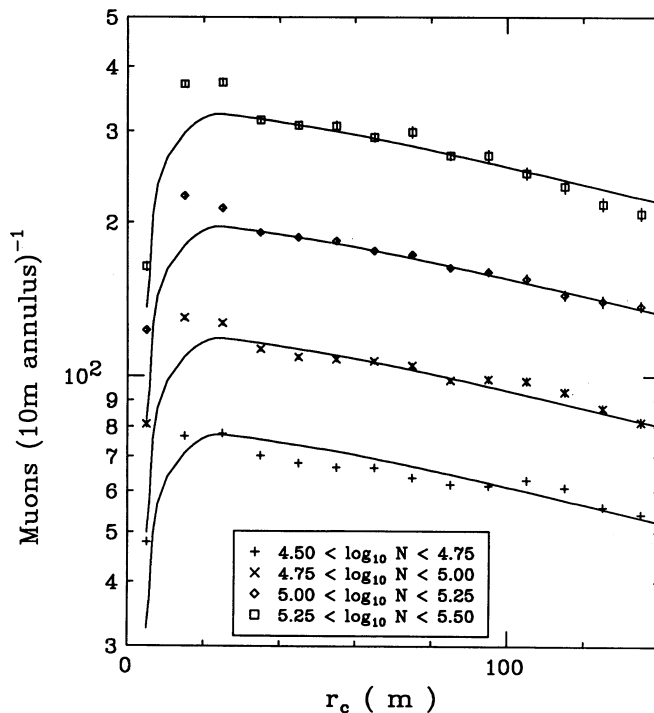


FIG. 2.—Lateral distributions of muons for cosmic-ray showers within  $5^\circ$  of vertical. The different groups of data refer to showers with different sizes as measured by the counters on the surface. The points represent the average number of hits in the buried counters, accumulated in annular rings of width 10 m and distances  $r_c$  from the shower axis. The solid curves are calculated from the lateral distribution function of Greisen (eq. [2]) with a 10 m smearing of the function to account for errors in measuring positions of shower cores. Punch-through is evident as an excess of hits close to the core. The amount of punch-through increases with shower size.

buried counters for nearly vertical showers of different sizes. The shapes of these distributions are almost the same and agree with Greisen's function (eq. [2]). However, a small amount of electromagnetic and hadronic *punch-through* is evident close to the core, especially for large showers. In Figure 3 we make the same comparison for two groups of showers, one within  $5^\circ$  of the vertical and the other slanting at more than  $30^\circ$  to the zenith. The two distributions are nearly identical except for the region close to the core where there is evidence of punch-through in the vertical showers. We discuss the effects of punch-through on  $\gamma$ -ray discrimination in a later paragraph.

We parameterize the average number of muons in showers by

$$\langle \log_{10} N_\mu \rangle \equiv a + b \sec \theta + c \log_{10} N, \quad (3)$$

where  $\theta$  is the angle with respect to the zenith. The coefficients in expression (3) are determined separately for each data run of  $\sim 24$  hr duration. Average values for coefficients  $a$ ,  $b$ , and  $c$  are  $-0.98$ ,  $0.62$ , and  $0.82$ , respectively. The dependence on zenith angle arises because the electron and muon components of the shower develop differently as the shower progresses. Shower simulations show that for a fixed energy of primary cosmic ray, the number of electrons at the ground decreases rapidly with increasing zenith angle while the number of muons decreases relatively slowly.

The muon content of individual showers fluctuates about the mean value given by expression (3). We define the *relative*

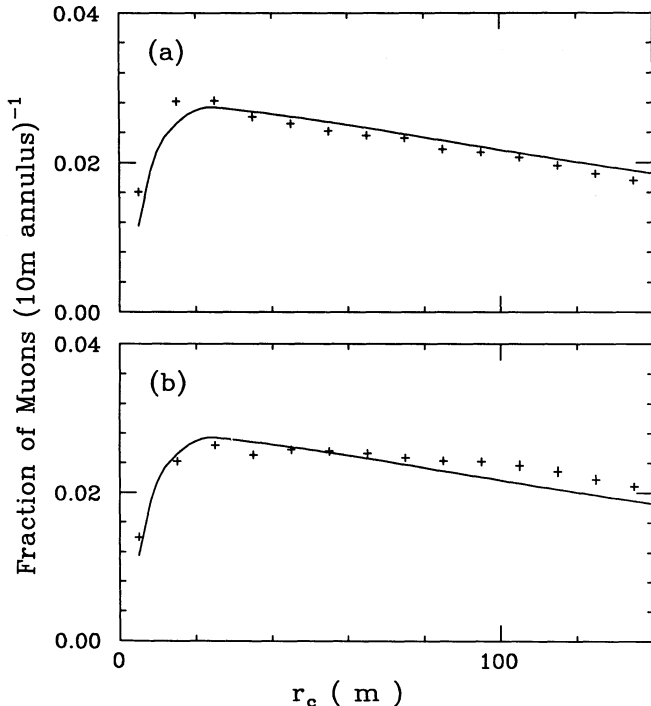
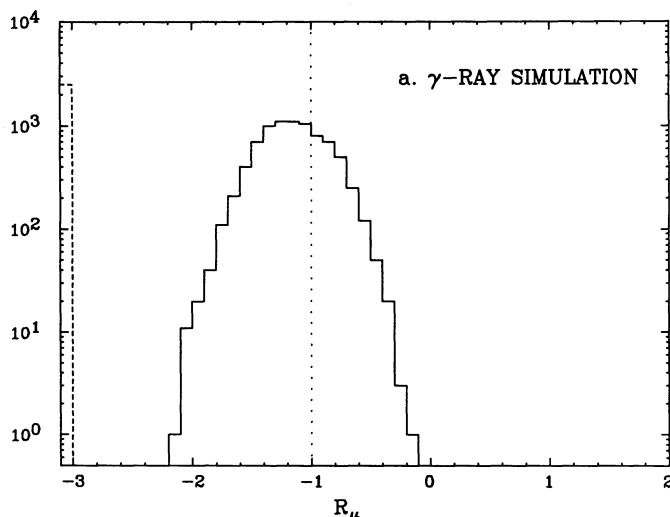


FIG. 3.—Lateral distributions of muons as measured by accumulated hits in the buried counters (a) for showers within  $5^\circ$  of the zenith and (b) for showers slanting at more than  $30^\circ$  to the zenith. The points represent the fraction of the total number of buried counter hits accumulated in annular rings of width 10 m and distances  $r_c$  from the shower axis. Error bars are slightly less than the size of the plot symbols. The solid curves are calculated from the lateral distribution function of Greisen (eq. [2]) with a 10 m smearing of the function to account for errors in measuring positions of shower cores. The distributions contain showers with  $N > 3 \times 10^4$ . Punch-through is evident as an excess of hits close to the core. The amount of punch-through decreases at large zenith angles due to increased absorption in air and earth.

muon size  $R_\mu$  of individual showers as

$$R_\mu \equiv \log_{10} N_\mu - \langle \log_{10} N_\mu \rangle. \quad (4)$$

The distribution of this quantity is shown in Figure 4. Fluctuations in  $R_\mu$  correspond to a full width at half-maximum of 0.52.



Air showers caused by  $\gamma$ -rays can mimic those caused by hadronic primaries if enough electrons penetrate to the buried array and are counted as muons. Since the electromagnetic component of an ordinary hadronic shower is similar to a  $\gamma$ -ray-induced shower, the characteristics of punch-through can be investigated by studying ordinary cosmic-ray events. We have measured the extent to which the muons we detect may be contaminated by punch-through by studying the lateral distribution of hits in the buried counters in our data.

The most energetic electrons in a hadron shower have a much narrower lateral distribution than the muons. Punch-through would reveal itself as an anomaly near the cores of large showers when compared with smaller showers. Evidence for such an effect can be found in Figure 2 where an excess of particles near the core is obvious for showers of size  $N \gtrsim 10^5$ . The excess is very small when compared to the total number of muons in the shower:  $\sim 2\%$  of the muons for showers with  $N = 10^5$  and  $\lesssim 1\%$  for showers with  $N = 3 \times 10^4$ . Punch-through is also reduced for slanting showers (Fig. 3), when compared with vertical showers of the same primary energy, because of increased absorption in the air and earth. We note that the above estimates include hadronic punch-through, which is negligible for  $\gamma$ -ray-induced showers. Based on the expected muon size of  $\gamma$ -showers (discussed below), we conclude that a negligible fraction of  $\gamma$ -rays will be misidentified because of electromagnetic punch-through.

#### 4. LIMITS ON THE $\gamma$ -RAY FLUX

We select individual air showers as candidates for  $\gamma$ -ray-induced showers when the muon size is less than 1/10 the average for ordinary hadronic showers of similar size and zenith angle. Specifically, we accept showers with  $R_\mu < -1.0$  as candidates. If UHE  $\gamma$ -rays interact in a conventional manner, virtually all  $\gamma$ -showers would meet this criterion except for errors introduced by the fitting procedure on showers with very low muon content.

Figure 4a displays the results of simulating the array's response to  $\gamma$ -ray-induced air showers (Kolodziejczak 1990). The events were generated according to an  $E_\gamma^{-1.7}$  integral primary energy spectrum, and the interaction model represents conventional photoproduction of muons. We find that 80% of

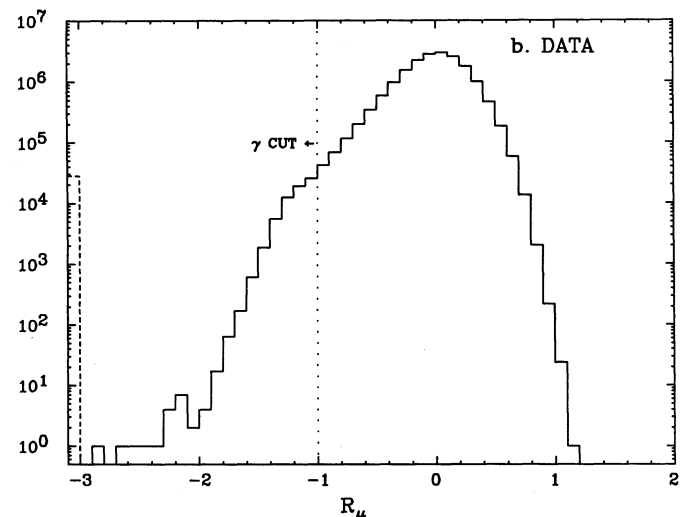


FIG. 4.—Distribution of the relative muon size  $R_\mu$  (eq. [4]) for (a) simulated  $\gamma$ -ray showers and (b) data. Eighty percent of simulated  $\gamma$ -ray events have  $R_\mu < -1.0$ , shown by the dotted line. Data with  $R_\mu < -1.0$  (i.e., to the left of the dotted line) are retained as candidate  $\gamma$ -ray showers. In each figure, showers with no recorded muons are plotted as underflows in the dashed bin at the left.



$\gamma$ -showers with  $N > 3 \times 10^4$  satisfy the  $R_\mu < -1.0$  criterion, rising to 90% for  $N > 10^5$ .

We first search for an isotropic flux of  $\gamma$ -rays by examining the data for evidence of an enhanced muon-poor component, regardless of direction. A more sensitive search is then made for  $\gamma$ -rays from the Galactic disk by comparing the muon content of showers from this direction with data from other regions of the sky. Finally, we apply the same technique to search for emission from smaller portions of the Galactic plane and several molecular clouds.

#### 4.1. Isotropic Diffusion Emission

Figure 4b displays the distribution of relative muon sizes  $R_\mu$  for data from 1988 April 3 until 1990 February 20 ( $1.9 \times 10^7$  events). Showers with no recorded muons are plotted as underflows in the dashed bin at the left. These and the other events in the  $R_\mu < -1.0$  region are mainly small showers ( $N \approx 3 \times 10^4$ ). The fluctuation of the muon size for small hadronic cosmic-ray showers is substantial and the shape of the curve is in accord with simulations of proton-induced cascades and muon-counting statistics in the detector. We set the most conservative limits on the isotropic flux of  $\gamma$ -rays by taking *all* showers with  $R_\mu < -1$  as candidates. The ratio of  $\gamma$ -rays to the total cosmic-ray flux is then  $I_\gamma/I_{\text{CR}} < 4.3 \times 10^{-3}$  (90% CL) for  $E_\gamma > 200$  TeV. If we consider the most energetic showers ( $N > 3 \times 10^5$ ,  $E_\gamma > 1000$  TeV), the above limit is lowered to  $I_\gamma/I_{\text{CR}} < 4.8 \times 10^{-4}$  (90% CL). These limits were obtained using data taken with eight patches of muon counters operating.

Our sensitivity to  $\gamma$ -rays could be further improved by estimating the expected number of showers with  $R_\mu < -1$  due to the expected downward fluctuations of muon size in ordinary cosmic-ray showers. Simple extrapolations of the observed  $R_\mu$  distribution from its peak region to the muon-poor tail would permit upper limits on  $I_\gamma/I_{\text{CR}}$  of less than  $10^{-4}$ . However, estimations of the shape of the  $R_\mu$  distribution are highly dependent upon assumptions regarding the composition of the primaries and the probability of large fluctuations in muon size. We merely note here that our simulations of the detector's response to proton showers shows qualitative agreement with the shape of the  $R_\mu$  distribution for  $R_\mu < 0$ . It is not necessary to include *any*  $\gamma$ -rays in the cosmic radiation to explain the data.

#### 4.2. Galactic Diffuse Emission

We search for enhanced Galactic  $\gamma$ -ray emission by comparing the muon content of showers from the direction of the Galactic plane with all other events ("non-Galactic" events). This method is more sensitive than the one employed above for isotropic  $\gamma$ -rays since we search for enhancements of the Galactic  $R_\mu$  distribution above expectations derived from non-Galactic data.

We define the Galactic disk here by Galactic latitudes  $|b^{\text{II}}| < 10^\circ$ . Because of our northern latitude, this sample of events is mainly from the region  $30^\circ < l^{\text{II}} < 220^\circ$  in Galactic longitude and does not include the Galactic center.

Figure 5 shows the  $R_\mu$  distributions separately for Galactic and non-Galactic showers. Galactic data are shaded. In each sample, events with no recorded muons are shown in the leftmost underflow bin. The non-Galactic sample has  $\sim 4$  times as many events as the Galactic data. There is no evidence for excess muon-poor showers either from the Galactic disk or non-Galactic directions. Both distributions exhibit a similar

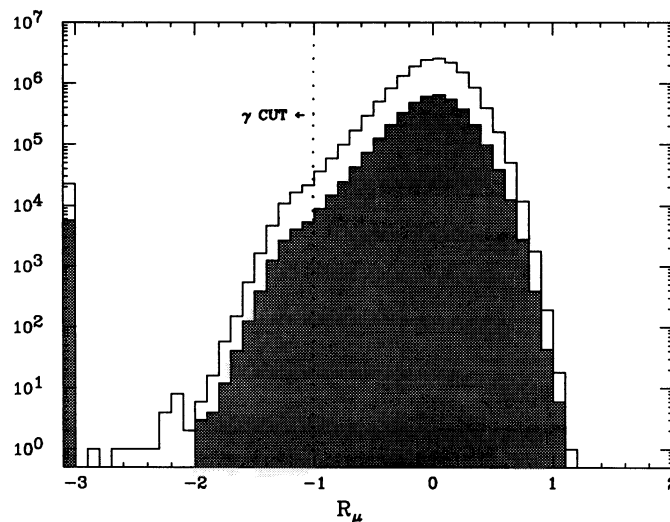


FIG. 5.—Distribution of relative muon size  $R_\mu$  (eq. [4]) as in Fig. 4b, except here the data are divided into two groups: Galactic (*shaded area*) and non-Galactic events. Showers with no recorded muons are plotted as underflows in the leftmost bin. Events with  $R_\mu < -1.0$  (i.e., to the left of the dotted line) are retained as candidate  $\gamma$ -ray showers.

"tail" of muon-poor showers. Since the vast majority of showers in each set are hadron induced, we predict the expected background of muon-poor showers in the Galactic data by scaling the non-Galactic distribution so that the number of showers with  $R_\mu > 0$  is the same in both samples.

We observe 19537 muon-poor showers from the Galactic disk and expect  $19503 \pm 71$ . With 90% confidence, there are less than 249 excess muon-poor showers from the total Galactic sample of  $3.9 \times 10^6$  events. The ratio of  $\gamma$ -ray showers to cosmic rays is then

$$\frac{I_\gamma}{I_{\text{CR}}} < \frac{249}{0.8 \times (3.9 \times 10^6)} = 8.0 \times 10^{-5}$$

for  $E_\gamma > 200$  TeV and directions within  $10^\circ$  of the Galactic plane. Similar limits are obtained when the data are restricted to higher energies.

Berezinsky & Kudryavtsev (1990, 1988) have recently calculated the flux of  $\gamma$ -rays arising from cosmic-ray interactions on gas and dust in the Galactic disk and predict  $I_\gamma/I_{\text{CR}} = 6.4 \times 10^{-5}$  for  $E_\gamma > 100$  TeV from the direction of the Galactic center. Our limit is very close to this prediction.

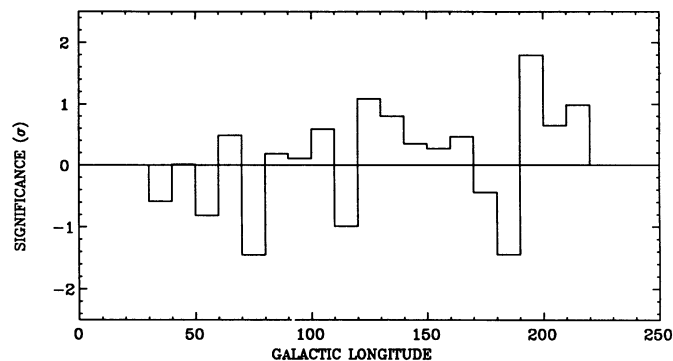


FIG. 6.—Significance of observed number of muon-poor showers with respect to the expected number along the Galactic plane ( $|b^{\text{II}}| < 10^\circ$ ). The bin size is  $\Delta l^{\text{II}} = 10^\circ$ . The significance is expressed in units of Gaussian standard deviation  $\sigma$ , calculated as in Li & Ma (1983).

TABLE 1  
OBSERVATIONS OF SELECTED MOLECULAR CLOUDS AND THE CENTRAL GALAXY

OBJECT	COORDINATES		AREA (deg <sup>2</sup> )	MASS (10 <sup>4</sup> M <sub>⊙</sub> )	DISTANCE (kpc)	E <sub>γ</sub> <sup>a</sup> (10 <sup>14</sup> eV)	PREDICTED <sup>b</sup> γ-RAY FLUX > E <sub>t</sub> (10 <sup>-14</sup> cm <sup>-2</sup> s <sup>-1</sup> )	I <sub>γ</sub> /I <sub>CR</sub> (90% CL upper limit) (10 <sup>-4</sup> )	γ-RAY FLUX > E <sub>t</sub> (90% CL upper limit) (10 <sup>-14</sup> cm <sup>-2</sup> s <sup>-1</sup> )
	l <sup>II</sup>	b <sup>II</sup>							
Cas OB6 .....	135°	2°	28	10	2.0	3.0	0.021	< 3.8	< 0.87
Per OB2 .....	157	-21	28	4	0.35	2.0	< 0.03	< 9.6	< 4.1
Cygnus .....	80	3	28	70	1.7	2.0	0.15	< 6.2	< 2.7
Taurus .....	172	-15	100	2	0.14	2.5	0.026	< 4.0	< 3.8
"Central" Galaxy .....	30-40	±10	200	?	~10	11.0	0.20	< 9.6	< 1.5

<sup>a</sup> The energy threshold  $E_t$  depends primarily upon declination of the object.

<sup>b</sup> The predicted flux is an extrapolation of satellite observations at 0.1 GeV (see text).

### 4.3. Molecular Cloud Emission

Satellite observations reveal that the intensity of low-energy ( $> 30$  MeV)  $\gamma$ -rays varies along the Galactic plane. To the extent that these  $\gamma$ -rays are products of interactions of cosmic rays with gas and dust, the variation is due to nonuniformities of the interstellar medium. Consequently, we expect that UHE  $\gamma$ -rays should have a similar spatial structure. We have looked in detail at specific regions of the Galaxy using the method of muon discrimination described above.

Figure 6 compares the observed number of muon-poor showers with the number expected from fluctuations of ordinary cosmic rays. We have divided the Galactic plane into bins of longitude  $\Delta l^I = 10^\circ$  having latitude  $|b^II| < 10^\circ$ . The significance of the difference between the observed number of showers and the expected number is expressed as a Gaussian standard deviation  $\sigma$ , computed according to the prescription of Li and Ma (1983). The expected number of muon-poor showers is computed from non-Galactic data, as described in § 4.2. We find no significant excess emission of muon-poor showers from any part of the Galactic plane visible to the detector.

Table 1 lists four northern hemisphere molecular clouds which are sources of  $\gamma$ -rays with  $E_\gamma > 0.1$  GeV (Issa & Wolfendale 1981). We have also included a 200 deg<sup>2</sup> region of the central Galactic plane for the interval  $30^\circ < l^I < 40^\circ$  (The acceptance of our apparatus drops off very rapidly below  $l^I = 30^\circ$ ). The listed areas of the objects are the sizes of the acceptance windows used in the analysis. These are, in some cases, larger than the actual size of the objects because we use a minimum acceptance half-angle of  $3^\circ$ .

The energy threshold varies according to the mean zenith angle of the source at our location. For purposes of comparison we have extrapolated the satellite results to our energy threshold using a  $E_\gamma^{-1.5}$  integral power law. The resulting "predicted" fluxes are given in Table 1. The mechanism(s) that generate the low-energy  $\gamma$ -rays in these objects are not entirely understood, so firm predictions of the UHE flux cannot be given. The  $E_\gamma^{-1.5}$  power law may be optimistic or pessimistic.

No significant excess signals are seen from any of the objects listed. We compute limits on the ratio  $I_\gamma/I_{CR}$  as described in the

previous section and obtain the corresponding flux using the all-particle cosmic-ray intensity  $I_{CR}$  given by Protheroe (1987). We have included a factor which estimates the loss of signal due to reconstruction errors. The last column of Table 1 gives our 90% CL flux limits. The upper limits we observe are generally larger than the "predicted" values. A detector with at least 10 times the sensitivity of our present device is required in order to detect UHE  $\gamma$ -rays from these sources.

### 5. SUMMARY AND DISCUSSION

We find no evidence for an isotropic  $\gamma$ -ray component nor for an enhanced  $\gamma$ -flux from the Galactic plane. Above 200 TeV, the contribution of  $\gamma$ -rays to the total cosmic-ray flux is less than 0.4% (90% CL); above 1000 TeV, this ratio is less than 0.05%. Any additional  $\gamma$ -rays from the Galactic disk comprise less than  $8.0 \times 10^{-5}$  (90% CL) of the total cosmic-ray intensity from this direction.

Discrimination of  $\gamma$ -showers based on muon content is a powerful technique. This observational limit on Galactic  $\gamma$ -rays is nearly two orders of magnitude below previous experiments and approaches the level predicted theoretically. If  $\gamma$ -ray showers are indeed muon-poor, the Galactic  $\gamma$ -ray flux may become observable with continued observation.

In the future, we anticipate improved sensitivity to diffuse Galactic  $\gamma$ -rays. The surface counter array used in the present study has been replaced by the Chicago Air Shower Array (Ong 1990) and the muon array is being expanded. The final configuration of the UMC experiment will increase the rate of collection of air showers tenfold and double the size of the muon array described here. The muon discrimination ability of the full UMC array will be roughly the same as in the present analysis. We expect a factor of 3 improvement in sensitivity to Galactic  $\gamma$ -rays in about one live-year operation, due mainly to the higher data collection rate.

The authors gratefully acknowledge the help and support of our colleagues at the University of Chicago and Colonel J. A. Van Prooyen and the staff of Dugway Proving Ground. This work was supported in part by the US Department of Energy and the National Science Foundation.

### REFERENCES

- Berezinsky, V. S., & Kudryavtsev, V. A. 1988, *Soviet Astr. Letters*, 14, 370  
 ———, 1990, *ApJ*, 349, 620  
 Ciampa, D., et al. 1990, *Phys. Rev.*, D42, 281  
 Clay, R. W., Protheroe, R. J., & Gerhardy, P. R. 1984, *Nature*, 309, 687  
 Greisen, K. 1960, *Ann. Rev. Nucl. Part. Sci.*, 10, 63  
 Halzen, F., et al. 1990, *Phys. Rev.*, D41, 342  
 Hartman, R. C., et al. 1979, *ApJ*, 230, 597  
 Issa, M. R., & Wolfendale, A. W. 1981, *Nature*, 292, 430  
 Kolodziejczak, J. 1990, Ph.D. thesis, University of Michigan (unpublished)  
 Li, T. P., & Ma, Y. Q. 1983, *ApJ*, 272, 317  
 Mayer-Hasselwander, H. A., et al. 1982, *A&A*, 105, 164  
 Nikolsky, S. I., Stamenov, J. N., & Ushev, S. Z. 1987, *J. Phys. G: Nucl. Phys.*, 13, 883  
 Ong, R. A. 1990, *Nucl. Phys. B (Proc. Suppl.)*, 14A, 273

Protheroe, R. J. 1987, Proc. 20th Internat. Cosmic Ray Conf. (Moscow), 8, 21  
Reynolds, P. T., et al. 1990, Proc. 21st Internat. Cosmic Ray Conf. (Adelaide),  
2, 383  
Samorski, M., & Stamm, W. 1983, Proc. 18th Internat. Cosmic Ray Conf.  
(Bangalore), 11, 244

Sinclair, D. 1989, Nucl. Instr. Meth., A 278, 583  
Suga, K., et al. 1988, ApJ, 326, 1036  
Yoshida, S., & Teshima, M. 1990, Proc. 21st Internat. Cosmic Ray Conf.  
(Adelaide), 2, 403